PHYSICAL REVIEW C **71**, 051602(R) (2005)

Estimation of (n, f) cross sections by measuring reaction probability ratios

C. Plettner,[1] H. Ai,[1] C. W. Beausang,[1,2] L. A. Bernstein,[3] L. Ahle,[3] H. Amro,[1] M. Babilon,[1,4] J. T. Harke,[3] J. A. Caggiano,[1] R. F. Casten,[1] J. A. Church,[3] J. R. Cooper,[3] B. Crider,[2] G. Gürdal,[1,5] A. Heinz,[1] E. A. McCutchan,[1] K. Moody,[3] J. A. Punyon,[3] J. Qian,[1] J. J. Ressler,[1] A. Schiller,[6] E. Williams,[1] and W. Younes[3]

[1]*A. W. Wright Nuclear Structure Laboratory, Yale University, New Haven, Connecticut 06511*

[2]*Department of Physics, Richmond University, Richmond, Virginia 23173*

[3]*Lawrence Livermore National Laboratory, Livermore, California 94550*

[4]*Institut für Kernphysik, Technische Universität Darmstadt, D-64289, Germany*

[5]*Clark University, Worcester, Massachussetts 01610*

[6]*MSU/NSCL, 1 Cyclotron Road, East Lansing, Michigan, 48824*

(Received 18 January 2005; published 19 May 2005)

Neutron-induced reaction cross sections on unstable nuclei are inherently difficult to measure due to target activity and the low intensity of neutron beams. In an alternative approach, named the "surrogate" technique, one measures the decay probability of the same compound nucleus produced using a stable beam on a stable target to estimate the neutron-induced reaction cross section. As an extension of the surrogate method, in this paper we introduce a new technique of measuring the fission probabilities of two different compound nuclei as a ratio, which has the advantage of removing most of the systematic uncertainties. This method was benchmarked in this report by measuring the probability of deuteron-induced fission events in coincidence with protons, and forming the ratio $P[^{236}\mathrm{U}(d, pf)]/P[^{238}\mathrm{U}(d, pf)]$, which serves as a surrogate for the known cross section ratio of $^{236}\mathrm{U}(n, f)/^{238}\mathrm{U}(n, f)$. In addition, the $P[^{238}\mathrm{U}(d, d'f)]/P[^{236}\mathrm{U}(d, d'f)]$ ratio as a surrogate for the $^{237}\mathrm{U}(n, f)/^{235}\mathrm{U}(n, f)$ cross section ratio was measured for the first time in an unprecedented range of excitation energies.

DOI: 10.1103/PhysRevC.71.051602 PACS number(s): 25.85.Ge, 25.70.Gh, 25.85.Ec, 25.40.−h

Neutron-induced reaction cross sections on unstable nuclei play an important role in astrophysical nucleosynthesis and in extreme environments where neutron densities and temperatures are high, such as the interior of supernovae. In particular, measuring neutron-induced fission cross sections of actinide nuclei may shed some light on physical quantities such as fission barrier heights and level densities, and provide insight into the competition between fission and neutron emission. While the $^{233-236,238}\mathrm{U}$ neutron-induced fission cross sections are measured directly up to 400 MeV incident neutron energy [1,2], the $^{237}\mathrm{U}(n, f)$ case, because its half-life is only 6.8 days, falls into the category of very difficult experiments. Indeed, almost 30 years have elapsed since the last attempt to measure this cross section. In Ref. [3], only a few points were sampled with neutron energy around 200 keV. Data up to 2 MeV incident neutron energy are available from Ref. [4], where a nuclear explosion was used as the intense neutron source. A critical assembly measurement [5] yielded results that conflict with the data from Ref. [4]. It should be noted that, in general, the energy range for these measurements does not exceed 2 MeV incident neutron energy.

There is an alternative approach which circumvents the problems inherent in the direct measurement of cross sections of short-lived nuclei. In the surrogate technique, the neutron-induced reaction probability is estimated by measuring the reaction probability for the same compound nucleus formed by means of a different reaction using a stable beam and target. In the 1970s, the (t, pf) "surrogate" technique was employed in Refs. [6–9], where the measured (t, pf) reaction probability was used to deduce the (n, f) cross section by

$$\sigma_{(n,f)}(E_n) = \sigma_{\mathrm{CN}}(E_n) P_{(t,pf)}(E_x), \tag{1}$$

where $\sigma_{\mathrm{CN}}(E_n)$ is the compound nucleus formation cross section as a function of incident neutron energy E_n, and $P_{(t,pf)}(E_x)$ is the fission probability following the (t, p) compound nucleus formation at an excitation energy $E_x = E_n + B_n$, with B_n the neutron binding energy. Here, the cross section $\sigma_{\mathrm{CN}}(E_n)$ is obtained from an optical model calculation, while the probability $P_{(t,pf)}(E_x)$ is the measured quantity. However, the limitation of this technique is that the absolute reaction probability has to be measured ($P_{(t,pf)} = \frac{N_{(t,pf)}}{N_{(t,p)}}$), which relies largely on the accurate determination of the (t, p) events number $N_{(t,p)}$. This determination turns out to be the source of the largest uncertainty in the surrogate result, due to practical experimental problems of target contamination. In the current approach, the (d, xf) reaction, where x stands for a proton or deuteron, on $^{236,238}\mathrm{U}$ targets was used as a surrogate for the (n, f) reaction. The uncertainty of $N_{(d,d')}$ is eliminated in our method by using a ratio of probabilities of two reactions: $P_{(d,xf)}(^{238}\mathrm{U})/P_{(d,xf)}(^{236}\mathrm{U}) \sim N_{(d,xf)}(^{238}\mathrm{U})/N_{(d,xf)}(^{236}\mathrm{U})$. The (d, pf) deuteron-induced probability for $^{236,238}\mathrm{U}$ targets was used to benchmark the method, since it serves as a surrogate for the $^{236}\mathrm{U}(n, f)/^{238}\mathrm{U}(n, f)$ cross section ratio, where direct measurements are available [10]. Excellent agreement with the existing data was obtained. In addition, the deuteron-induced fission probability ratio for the $(d, d'f)$ reaction, which models

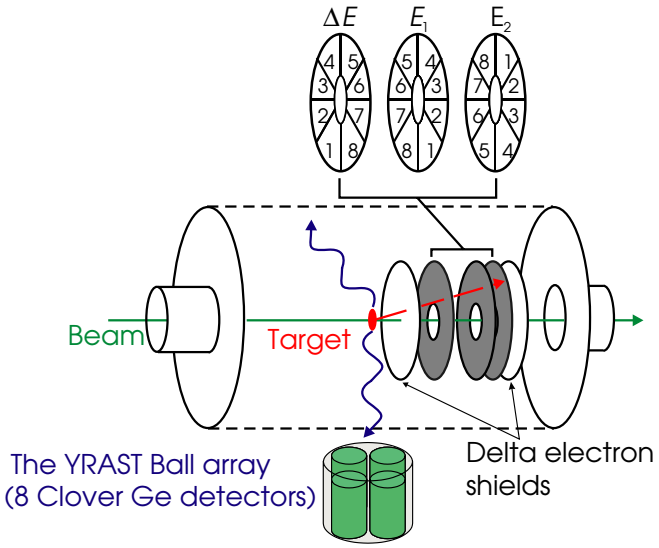

FIG. 1. (Color online) Schematic view of STARS, consisting of three segmented Si detectors with the first detector being the ΔE. The remaining two detectors are electronically connected and serve as the E detector. The sector orientation is also shown.

the ^{237}U$(n, f)/^{235}$U(n, f) cross section ratio, was obtained for equivalent neutron energies up to 14 MeV for the first time.

The ^{236,238}U targets were prepared as nitrates of approximately 300 μg/cm^2 thickness, "stippled" on a 200 μg/cm^2 carbon backing. Deuterium beams of 24 and 32 MeV energy were delivered by the ESTU tandem accelerator of Yale University. The average beam intensity amounted to 1 enA. Charged particles were detected using the STARS detector (silicon telescope array for reaction studies) [11], which was configured as a ΔE-E telescope; see Fig. 1. The telescope consisted of three "*S*2" type annular double-sided silicon (Si) detectors. The thickness of the front detector (ΔE) was 140 μm. The back detector (E) consisted of two Si detectors, E_1 and E_2, each of 1000 μm thickness. The thickness of the back detectors was such that the deuterons were fully stopped at a beam energy of 24 MeV. Each Si detector was segmented on one side into 48 rings and on the other side into 16 wedge-shaped segments. However, adjacent rings and sectors were electrically connected, so that for each detector a total of 24 rings and 8 sectors was recorded. The angular coverages, expressed as a percentage of 4π for the ΔE detector and the ΔE-E_1 and ΔE-E_2 pairs were 22.5, 16.5, and 9.5%, respectively. The detectors were protected from δ electrons by placing aluminum shields in front of and behind the telescope. The rear shield and the target were operated under voltages of +400 and +300 V, respectively. Thick (~2 cm) annular aluminum collimators were placed upstream of the target in the reaction chamber to prevent the incoming deuteron beam from damaging the detectors. To detect coincident γ radiation, an array of eight Compton suppressed clover detectors from the YRAST ball array [12] were arranged around the STARS reaction chamber at 90° with respect to the beam direction.

The energy and the time information for each ring and sector were digitized using VME analog-to-digital converters and time-to-digital converters (TDC). The range of the TDCs was 1.2 μs. In the subsequent analysis, prompt coincidence windows of 50 ns (for the E detector) or 120 ns (for the ΔE) were required. Approximately 65% of the events were rejected by this requirement. The master trigger was generated whenever a sector or a ring in the back detector (E_1 or E_2) fired. The master trigger rate was typically 40 kHz, while the total rate in the ΔE detector was 20 kHz.

The $(d, d'f)$ or (d, pf) events of interest are characterized by coincident deuteron (proton) and fission fragments. While the light-charged particles, deuterons and protons, are identified by their characteristic ΔE-E energy distribution, the fission fragments are fully stopped in the ΔE detector. Therefore, candidate fission fragments are identified by their prompt coincidence with a light-charged particle and by their energy deposition in the front detector. Hence, the selection of the $(d, d'f)$ or (d, pf) subset of events was made from those events with (i) two distinguishable hits in the front detector (one hit corresponding to the detection of the d' or p and the other corresponding to the detection of one of the fission fragments) and (ii) one hit in the back detector corresponding to the d' or p (in E_1 or E_2 or both, depending on the angle and on incident energy.) We note that the $(d, d'f)$ and (d, pf) events of interest represent only a small fraction of the total fission cross section, which is dominated by the (d, f) reaction (1:500). The goal was thus to extract a clean sample of $(d, d'f)$ and (d, pf) events from this background. The prompt time coincidence window and the establishment of the correct flight path correlation (between sectors and rings in the ΔE and E detectors) for the scattered light-charged particle, were vital for accomplishing this goal. The ring-ring correlations were determined from the known detector geometry and confirmed using the experimental data and Monte Carlo simulations of energy loss of protons and deuterons in Si detectors. The sector orientation for the ΔE, E_1, and E_2 detectors is schematically shown in Fig. 1. When a particular sector in the front detector is hit, the particle (mostly) also hits the back detector sector directly behind the front sector. Thus, a simple linear equation connecting the sector numbers [sector(ΔE) + sector(E_1) = 9] and [sector(E_1) + sector(E_2) = 5] or [sector(E_1) + sector(E_2) = 13] is adequate to describe their correlation.

Having established both the ring-ring and sector-sector correlations, ΔE-E matrices were created for each ring of the front detector that lies within the angular coverage of the back detector. An example of such a matrix is shown in Fig. 2. The various contributions of different charged particles are clearly visible on this plot. While the most energetic peak in the deuteron distribution is due to elastic scattering of deuterium on uranium, the other peaks are due to reactions on light-ion target contaminants, such as carbon, nitrogen, and oxygen. By setting individual polygon gates around the proton and deuteron distributions (as illustrated in Fig. 2 for the deuterons) in each ΔE-E matrix, coincident fission fragments in the ΔE detector associated with the (d, pf) or $(d, d'f)$ reaction could be selected, respectively. Such a spectrum of candidate fission fragment energies for the ^{238}U data is shown in Fig. 3(a). A significant background of low-energy events, originating from the light-ion target contamination, is still present. To estimate the influence of

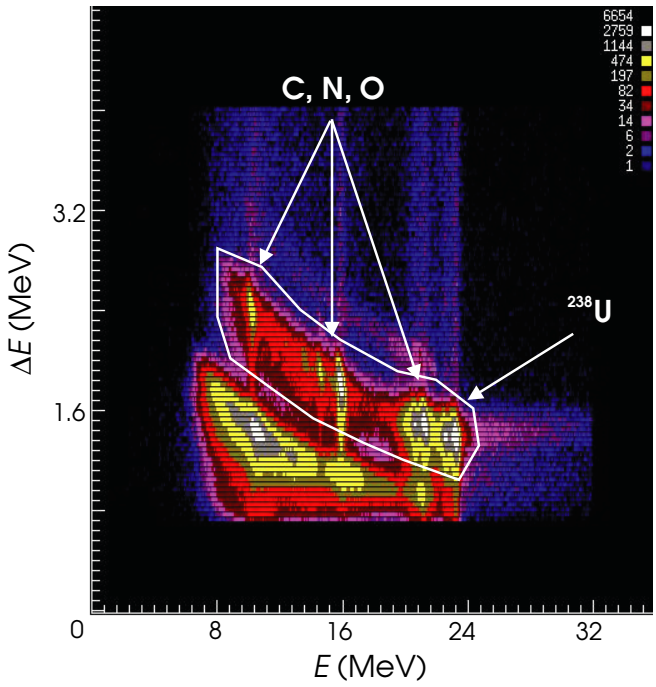

FIG. 2. (Color online) Particle identification ΔE-E spectrum for 24 MeV deuterons incident on a ^{238}U target with counts plotted on a logarithmic scale. The spectrum was recorded by ring no. 3 in the ΔE detector, which is located at 37.4° with respect to the beam. The distribution inside the polygon corresponds to deuterons, and the distribution below it corresponds to protons.

such events, data were also obtained using an ammonium nitrate target stippled onto a carbon backing (no fissionable nuclei). Applying the same sort of procedure to this target yields the spectrum shown in Fig. 3(b). It is clear that the light-ion background does not extend above ∼14 MeV and that the fraction of real fission events below this energy is small. In our subsequent analysis, only those candidate fission particles with energies greater than 14 MeV were assumed

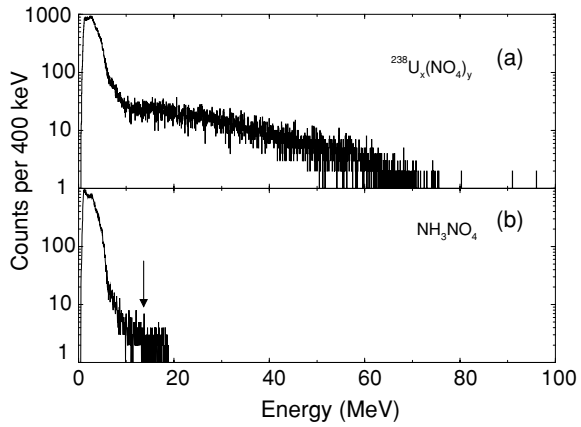

FIG. 3. Candidate fission energy spectrum extracted for the ^{238}U target (a), and a background spectrum obtained using a NH_3NO_4 target (b). Note that the most spurious fission events from reactions on the target contaminants stop at energy depositions of 14 MeV in the ΔE detector.

to be fission fragments. Finally, particle-fission timing was essential for removing the accidental contributions originating from the (d, f) background events. A gate on the prompt time window was set, and the contributions from the time random fission events (the off-prompt data) have been subtracted.

Figure 4 shows the number of fission events coincident with scattered protons plotted as a function of excitation energy of the compound nucleus, for both ^{236}U (a) and ^{238}U (b) nuclei. The compound nucleus excitation energy range of the measurement is limited by, on the low-energy side, by the proton "punch through" (maximum energy loss limit in the particle telescope), and on the upper energy side, by the Coulomb barrier for the ejectiles. For excitation energies larger than the fission barrier height (5.8 MeV for both ^{236}U and ^{238}U [13]), the number of fission events increases, as expected.

Having determined the number of fission events in coincidence with deuterons (protons) $N_{(d,d'f)}$ ($N_{(d,pf)}$), the probability of deuteron (proton)-induced fission can be obtained, provided that the denominator $N_{(d,d')}$ is known. The latter quantity cannot be accurately determined due to target contamination. To surpass this difficulty, a ratio of probabilities was formed instead:

$$\frac{P_{(d,d'f)}(^{238}\mathrm{U})}{P_{(d,d'f)}(^{236}\mathrm{U})} = \frac{N_{(d,d'f)}(^{238}\mathrm{U}) \times N_R(^{236}\mathrm{U}) \times W(^{236}\mathrm{U})(\theta)}{N_{(d,d'f)}(^{236}\mathrm{U}) \times N_R(^{238}\mathrm{U}) \times W(^{238}\mathrm{U})(\theta)}. \quad (2)$$

Here, N_R is the number of Rutherford scattered deuterons which accounts for differences in target thickness and beam intensities for the ^{236}U and ^{238}U experiments, while $W(\theta)$ is a correction factor for the angular correlation between the outgoing deuteron and the fission fragment. We note that, generally, the method of reporting ratios eliminates most of the systematic uncertainties, since the $N_{(d,d')}$ values are very similar for ^{236}U and ^{238}U and cancel out in the ratio. The Rutherford scattering was measured by integrating the yield of the elastic scattered deuterons in the total (d, d') spectrum. The contribution of Coulomb excitation to the elastic peak was estimated using two different methods and found to be negligible. First, a gate was placed on the elastic peak in the deuteron spectrum, and the coincident γ-ray spectrum was projected. The yield of low-lying excited states in the uranium spectrum was found to be very small. Second, a Winther–de Boer [14] calculation indicates that the ratio of Rutherford scattering to Coulomb excitation of the first few excited states in uranium is extremely large. Finally, the direct reaction cross sections to the first few excited states depend on mass number A, so they contribute with equal percentage to ^{236}U and ^{238}U, and the Rutherford ratio is not affected.

At low excitation energies, fission fragments show a strong angular correlation with respect to the ejectile [15]. These anisotropies are very similar for ^{236}U and ^{238}U, exhibiting at most a 4.6% difference [16]. At higher excitation energies, this anisotropy disappears as additional states become available above the fission barrier [17]. The 24 MeV $(d, d'f)$ events were the only data that required this correction since they extended down to the fission barrier. In order to take this into account, a Gaussian correction term was applied to the 24 MeV $(d, d'f)$ to gradually decrease the correction factor from the maximum (4.6%) near the fission barrier to zero near 9 MeV.

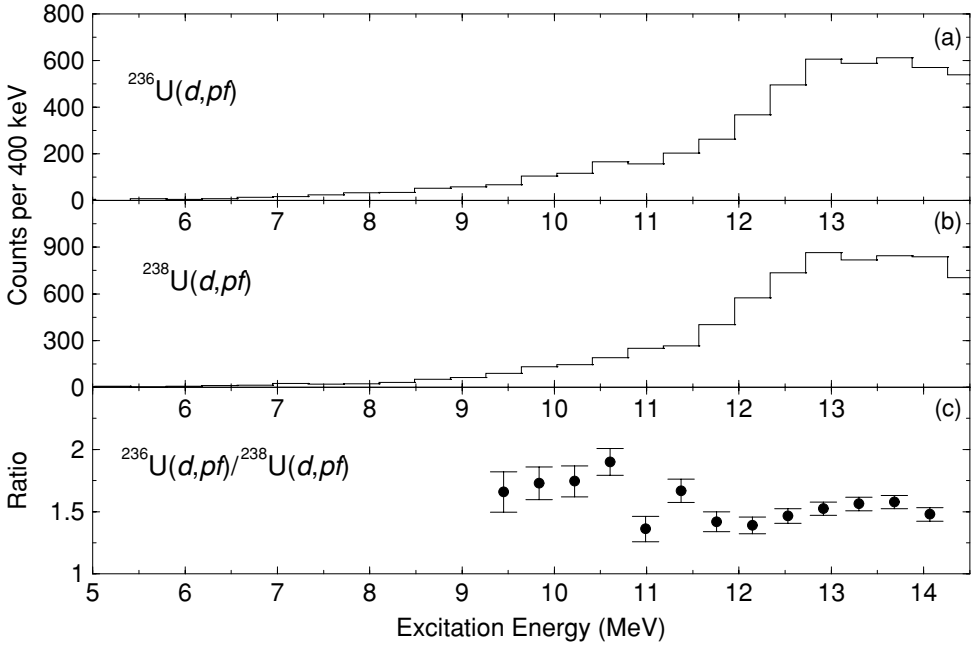

FIG. 4. Fission events coincident with protons for the (a) ^{236}U target, (b) ^{238}U, and (c) the ratio of (d, pf) events of ^{236}U/^{238}U, as a function of excitation energy in the compound nucleus. The data were obtained at 24 MeV incident deuteron energy.

We now consider the relationship between the surrogate deuteron-induced fission probability and the corresponding neutron-induced cross section. The compound nucleus formation cross section σ_{CN} is very similar for ^{238}U and ^{236}U, since these nuclei have similar structure, and the compound nucleus formation cross sections scale as $A^{2/3}$ [18]. Therefore, based upon Eq. (1), the compound nucleus formation cross section also cancels, leaving only the fission probability in the ratio. Thus, the neutron-induced cross sections ratio can be expressed as follows:

$$\frac{\sigma_{(n,f)}(^{238}\mathrm{U})(E_x)}{\sigma_{(n,f)}(^{236}\mathrm{U})(E_x)} = \frac{P_{(d,pf)}(^{238}\mathrm{U})(E_x)}{P_{(d,pf)}(^{236}\mathrm{U})(E_x)}. \quad (3)$$

It should be mentioned, however, that for excitation energies lower than 8 MeV in the actinides, the ratio is affected by differences in the angular momentum distributions excited in the direct reaction and the neutron capture reaction. For instance, the ground-state spins of ^{237}U and ^{235}U differ ($J^\pi = 1/2^+$ and $7/2^-$, respectively), and this can induce a 30% difference in the neutron-induced fission cross section [19]. For excitation energies higher than 8 MeV, the dependence on the J^π disappears, and this is the region where the ratio technique becomes robust.

The advantage of this method also relies on the insensitivity of the ratio to any preequilibrium effects for the (n, f) reaction. Suppose that the compound nucleus undergoes a preequilibrium reaction, and that the preequilibrium components of ^{238}U and ^{236}U compound nuclei vary by $\Delta\sigma_{\mathrm{PEQ}}$. Thus, the compound nucleus formation cross-section ratio $\sigma_{\mathrm{CN+PEQ}}$ becomes

$$\frac{\sigma_{\mathrm{CN+PEQ}}(^{238}\mathrm{U})}{\sigma_{\mathrm{CN+PEQ}}(^{236}\mathrm{U})} = \frac{\sigma_{\mathrm{CN}}(^{238}\mathrm{U}) + \sigma_{\mathrm{PEQ}}(^{238}\mathrm{U}) + \Delta\sigma_{\mathrm{PEQ}}}{\sigma_{\mathrm{CN}}(^{236}\mathrm{U}) + \sigma_{\mathrm{PEQ}}(^{236}\mathrm{U})}. \quad (4)$$

For a difference of $\Delta\sigma_{\mathrm{PEQ}}$ of 20%, and small values of σ_{PEQ} [20], the ratio varies by 1–2% only, thus it is left rather unaffected by preequilibrium effects.

To benchmark and test the technique, the $P(d, pf)$ ratio was analyzed. The ^{236}U(d, pf) and ^{238}U(d, pf) reactions serve as surrogates for the well known ^{236}U(n, f) and ^{238}U(n, f), respectively; thus, the corresponding ratio can be compared to direct measurements. In Fig. 4(c), the proton-induced fission probability ratio is illustrated, with the correction factors discussed above taken into account. Furthermore, the ratio is compared to the direct measurements in Fig. 5. The

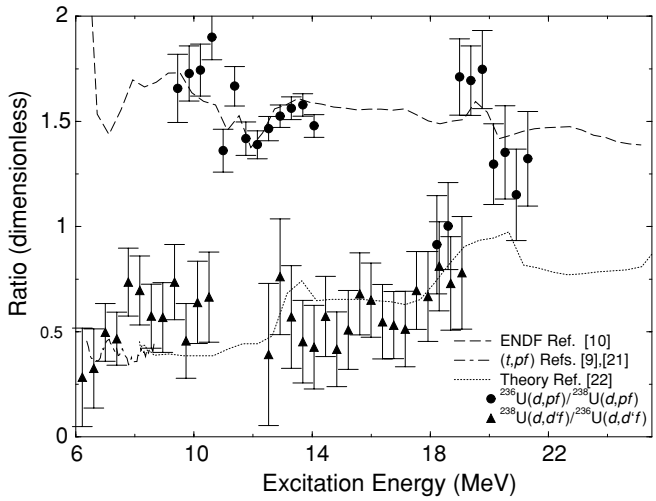

FIG. 5. Fission probability ratios for the (d, pf) and $(d, d'f)$ reactions on ^{238}U and ^{236}U targets, as a function of the excitation energy of the compound nucleus. The existing data and theoretical estimates are also indicated.

surrogate points follow closely the reported direct measurements [10], giving confidence in the measurement and the technique.

The $P_{(d,d'f)}$ ratio serves as a surrogate for the ^{237}U(n, f)/^{235}U(n, f) cross-section ratio, and since the ^{235}U(n, f) neutron-induced cross section is known, the ratio can be used to deduce the ^{237}U(n, f) cross section. In Fig. 5, these ratios are presented. The old low-energy surrogate data originating from the (t, pf) reaction [9,21], also plotted in Fig. 5, show good agreement with the STARS data. Our new measurement extends the ^{237}U(n, f) cross section to much higher energies, to $\sim$14 MeV equivalent neutron energy. A theoretical estimate [22] based on an extrapolation of the surrogate data obtained previously is also indicated on the graph, and the data match this prediction within 1σ accuracy. We note that this is the first measurement of the neutron-induced fission probability on ^{237}U over this energy range.

In conclusion, we have investigated the (d, xf) reactions on ^{236}U and ^{238}U targets employing the STARS detector. Reporting the results as a ratio of fission probabilities has the advantage of removing most of the systematic uncertainties associated with the measurement of absolute cross sections, and most of the sensitivity to preequilibrium effects. Our method was benchmarked using the fission probability ratio $P[^{236}\text{U}(d, pf)]/P[^{238}\text{U}(d, pf)]$ as a surrogate for the well known ^{236}U(n, f)/^{238}U(n, f) cross-section ratio. Excellent agreement over a wide range of excitation energy was found with the existing direct measurement data. As a first application of this technique, the ratio of fission probabilities $P[^{238}\text{U}(d, d'f)]/P[^{236}\text{U}(d, d'f)]$, as a surrogate for the ^{237}U(n, f)/^{235}U(n, f) cross-section ratio, was extracted from the same data set. The present data attempt to quantify the hitherto unknown ^{237}U(n, f) cross section with respect to the known ^{235}U(n, f) over an unprecedented range of incident neutron energies. However, more precision is needed, and future experiments, employing an α beam instead of deuterons, are expected to provide it. The method of reporting fission probabilities in two different compound nuclei (yet close in mass and similar in structure) as ratios turns out to be robust, model independent, and free from most systematic errors, and it can have broader applications, not only for actinides, but also in other regions of the nuclidic chart.

The assistance of J. Baris with data taking and of the staff of the ESTU accelerator at WNSL is very much appreciated. This work was supported by U.S. DOE research Grant Nos. DE-FG02-91ER-40609, DE-FG03-03NA-00081, DE-FG-02-88ER-40417, and W-7405-ENG-48 (LLNL), and by the Yale University Flint Fund.

[1] P. W. Lisowski, J. L. Ullman, S. J. Balestrini, A. D. Carlson, O. A. Wasson, and N. W. Hill, in *Proceedings of 50 Years with Nuclear Fission, Washington, D. C. and Gaithersburg, Maryland, 1989* (American Nuclear Society, La Grange Park, 1989), p. 443.

[2] P. W. Lisowski, A. Gavron, W. E. Parker, J. L. Ullmann, S. J. Balestrini, A. D. Carlson, O. A. Wasson, and N. W. Hill, in *Proceedings of Nuclear Data for Science and Techology, Jülich, Germany, 1991* (Springer-Verlag, Berlin, 1992), p. 268.

[3] G. A. Cowan, G. A. Jarvis, G. W. Knobeloch, and B. Warren, LASL Report LA-1669, 1955 (unpublished).

[4] J. H. McNally, J. W. Barnes, B. J. Dropesky, P. A. Seeger, and K. Wolfsberg, Phys. Rev. C **9**, 717 (1974).

[5] D. W. Barr (private communication).

[6] H. C. Britt, F. A. Rickey, and W. S. Hall, Phys. Rev. **175**, 1525 (1968).

[7] J. D. Cramer and H. C. Britt, Phys. Rev. C **2**, 2350 (1970).

[8] H. C. Britt and J. D. Cramer, Phys. Rev. C **2**, 1758 (1970).

[9] J. D. Cramer and H. C. Britt, Nucl. Sci. Eng. **41**, 177 (1970).

[10] Cross Section Evaluation Working Group, National Nuclear Data Center, Report BNL-NCS-17541 (ENDF-201), 1991 (unpublished).

[11] L. A. Bernstein *et al*., Proceedings of Nuclear Data for Science and Technology, Santa Fe, 2004 (in press).

[12] C. W. Beausang *et al*., Nucl. Instrum. Methods Phys. Res. A **452**, 431 (1997).

[13] W. D. Myers and W. J. Swiatecki, Nucl. Phys. **A81**, 1 (1966).

[14] A. Winther and J. de Boer, in *Coulomb Excitation*, edited by A. Winther and J. de Boer (Academic, New York, 1966).

[15] K. L. Wolf, R. Vandenbosch, and W. D. Loveland, Phys. Rev. **170**, 1059 (1968).

[16] R. F. Reising, G. L. Bate, and J. R. Huizenga, Phys. Rev. **141**, 1350 (1966).

[17] H. C. Britt and F. Plasil, Phys. Rev. **144**, 1046 (1966).

[18] J. Raynal, code ECIS95 (unpublished).

[19] W. Younes and H. C. Britt, Phys. Rev. C **67**, 024610 (2003).

[20] H. Feschbach, A. Kerman, and S. Koonin, Ann. Phys. (NY) **125**, 429 (1980).

[21] W. Younes and H. C. Britt, Phys. Rev. C **68**, 034610 (2003).

[22] W. Younes, H. C. Britt, J. A. Becker, and J. B. Wilhelmy, UCRL-ID-154194, 2003 (unpublished).